https://doi.org/10.5194/egusphere-2026-2115
Preprint. Discussion started: 12 May 2026

Effect of vibration on the elastic modulus of compacted Antarctic snow near Zhongshan Station

Fan Zhang[1], Tong Han[1], Qiming Zhang[1], Hao Wang[1], Zhenxuan Yin[1], Yihe Wang[1, 2], Biao Hu[2], Xueyuan Tang[2], Bo Sun[2], Enzhao Xiao[2]

[1] State Key Laboratory of Ocean Sensing & Ocean College, Zhejiang University, Zhoushan, 316021, China
[2] R & D Division of Polar Snow and Ice Runways, Polar Research Institute of China, Shanghai, China

Correspondence to: Enzhao Xiao (xiaoenzhao@pric.org.cn)

Abstract. As one of the fundamental mechanical properties of snow, the elastic modulus is critical to the design and construction of Antarctic snow runways and roads. While previous studies measured and investigated snow's elastic modulus through various experimental methods, the effects of vibratory treatment, a construction measure proven to enhance snow hardness, on the elastic modulus and the underlying mesoscale mechanism remain unexamined. This study investigates the vibration-induced effect on elastic modulus of compacted Antarctic snow near Zhongshan Station and the corresponding mesoscale mechanism. P-wave propagation experiments were conducted to measure the elastic modulus of vibrated and non-vibrated compacted Antarctic snow, and X-ray tomography imaging was employed to obtain the microstructures of vibrated and non-vibrated snow samples. Results show that for isothermal sintering of 48 hours at -10°C, vibratory treatment increases the elastic modulus by 83.13% while maintaining the snow density of 0.6 g/cm³ unchanged. At the mesoscale, vibratory treatment effectively homogenizes the pore space distribution within the ice matrix. Quantitative analysis revealed the following microstructural modifications: a 7.14% decrease in the mean structure thickness accompanied by a 12.41% reduction in the standard deviation, a 13.68% decrease in the mean pore thickness with a more pronounced 30.43% decline in the standard deviation, an 18.82% elevation in the minimum cut density, and a 2.09% enhancement in the directional connectivity. The findings provide theoretical support for rapid construction techniques of Antarctic snow runways and roads.

Key words: Elastic modulus; Antarctic snow; Vibration effect; Mesoscale mechanism.

1 Introduction

Compacted snow runways and roads, serving as the core components of Antarctica's transportation system, play a vital role in supporting the logistics of scientific expeditions across the continent. As these runways and roads are designed as multi-layered elastic structures, research on the elastic modulus, a key mechanical parameter of snow, holds significant importance for optimizing the design and construction of compacted snow runways and roads (Abele, 1990; Haehnel, 2019; Lang, 1997). Most experiments measuring the elastic modulus of snow were conducted under controlled laboratory conditions. Early studies employed quasi-static methods to determine the elastic modulus. Mellor (1975) summarized various studies by low-strain-rate

https://doi.org/10.5194/egusphere-2026-2115
Preprint. Discussion started: 12 May 2026

uniaxial compression tests, while Scapozza (2004) obtained similar results through quasi-static triaxial compression tests. However, due to snow's non-purely elastic behaviour, such methods inherently included viscoplastic strain components, yielding only an effective elastic modulus (Narita, 1980; Schweizer, 1998). Sigrist (2006) measured the elastic modulus through high-strain-rate dynamic loading experiments, and this method inherently circumvented snow's viscoplastic effects. Additionally, snow's elastic modulus can be derived through measurements by the SnowMicroPen (SMP) (Marshall & Johnson, 2009; Reuter et al., 2013). However, owing to the method's (Johnson & Schneebeli, 1999) lack of a sound theoretical justification, the calculated modulus values ultimately approximated those from quasi-static experiments. Among existing methods, P-wave propagation measurements were recognized as the most precise technique for determining snow's elastic modulus due to their high-frequency and low-amplitude characteristics (Mellor, 1975). For snow of identical density, the elastic modulus values obtained through this method exceeded those derived from the aforementioned experimental approaches (Capelli et al., 2016; Smith, 1965). Schneebeli (2004) pioneered a method to calculate snow's elastic modulus using finite element analysis based on three-dimensional microstructures reconstructed from computed tomography (CT) scans. Since then, this approach has been widely adopted in elastic modulus computations (Chandel et al., 2014; Srivastava et al., 2016; Wautier et al., 2015; Yuan et al., 2010). Gerling et al. (2017) employed P-wave propagation experiments under controlled laboratory conditions to measure snow's elastic modulus and compared the results with finite element analysis based on microstructural data from X-ray tomography images, validating the strong agreement between the two methods.

Density is generally regarded as a first-order factor controlling the elastic modulus of snow, yet it does not sufficiently represent the underlying microstructure (Frolov and Fedyukin, 1998). This is evident from the substantial scatter in reported elastic modulus values for snow samples with similar densities (Mellor, 1975; Narita, 1980; Schweizer, 1998; Scapozza, 2004; Sigrist, 2006; Gerling et al., 2017). To explain this discrepancy, a number of studies have introduced mesoscale descriptors beyond density. One group of approaches focused on geometrical characteristics of the ice matrix, such as grain size, coordination number, and grain contact area, in order to link bond-scale morphology with mechanical behavior (Gubler, 1978; Flin et al., 2011; Shertzer and Adams, 2011; Theile and Schneebeli, 2011; Wang et al., 2012; Hagenmuller et al., 2013a; Hagenmuller et al., 2013b; Hagenmuller et al., 2014a). Another line of work used correlation-length-based descriptors to quantify anisotropy in the pore and ice phases and to incorporate this information into constitutive descriptions of snow elasticity (Srivastava et al., 2010; Löwe et al., 2013; Calonne et al., 2014; Srivastava et al., 2016). Hagenmuller et al. (2014) further proposed the minimum cut density to characterize the weakest cross-sections controlling force transmission. In addition, Hildebrand and Rüegsegger (1997) defined local thickness as the diameter of the largest sphere containing a given point and lying entirely within the phase of interest, and this metric has been widely used in snow research to characterize microstructural evolution, particularly during temperature-gradient metamorphism (Schneebeli and Sokratov, 2004; Pinzer, 2009). Recent work has further emphasized the mechanical significance of snow microstructure. Schöttner et al. (2026) showed that microstructure governs how density is translated into mechanical response, with stiffness being primarily associated with descriptors related to the alignment and efficiency of load-bearing paths. Xiao et al. (2026a) identified connected local force-transmitting channels in the loading direction as the necessary condition for load-bearing force chains in compacted Antarctic snow, and proposed

https://doi.org/10.5194/egusphere-2026-2115
Preprint. Discussion started: 12 May 2026

directional connectivity and structure thickness as relevant mesoscale indices for parameterizing elastic modulus. In addition, Xiao et al. (2026b) applied structure thickness, pore thickness, minimum cut density, and directional connectivity in the mesoscale analysis of the strengthening effect of mechanical vibration on the uniaxial compressive strength of compacted Antarctic snow, showing that these descriptors are effective for capturing vibration-induced microstructural modifications even under constant overall density.

On the other hand, previous engineering practice and field observations have long suggested that mechanical vibration can improve the mechanical performance of compacted snow layers. Foundational studies by Wuori (1959, 1960) established early principles for vibratory compaction of snow, and Wuori (1965) further showed that vibration could significantly increase snow hardness, with more pronounced effects when the interval between compaction and vibration was shorter. Abele (1990) also reported that, under specific conditions, vibratory treatment markedly enhanced snow hardness without significantly increasing snow density. More recently, Xiao et al. (2026b) demonstrated that mechanical vibration significantly increased the uniaxial compressive strength of compacted Antarctic snow while maintaining constant overall density. These findings suggest that the mechanical effects of vibration are not solely controlled by density changes. However, the effects of vibratory treatment on the elastic modulus of compacted Antarctic snow and the corresponding mesoscale mechanism have rarely been studied.

This paper investigates the effect of vibration on the elastic modulus of compacted Antarctic snow near Zhongshan Station and the underlying mesoscale mechanism. First, P-wave propagation experiments were conducted to measure the elastic modulus of vibrated (experimental group) and non-vibrated (control group) compacted Antarctic snow, while micro-computed tomography (μCT) scanning was employed to reconstruct the 3D microstructure of the snow samples. Afterwards, mesoscale indices including structure and pore thickness, minimum cut density and directional connectivity, were adopted to analyze the mesoscale mechanism of vibratory treatment.

2 Snow sample preparation and storage

This section presents the sample preparation process for P-wave propagation experiments and μCT scanning.

Figure 1 shows the flowchart of the snow sample preparation and P-wave experiment of this study. For the P-wave propagation experiments, natural snow collected from depths of 1–3 m near Zhongshan Station was fragmented into blocks using an ice crusher, followed by sieving to collect snow particles with diameters of 1–2 mm. The sieved snow particles were filled into metal molds and compacted layer by layer along the specimen height direction to a target density of 0.6 g/cm³. During compaction, the specimen density was controlled by fixing the snow mass added to each layer and the compaction thickness of each layer. The final size of each specimen was 50 × 50 × 120 mm. Compaction was carried out by manually striking a punch with a hammer, while the punch remained in direct contact with the top surface of the snow specimen. Each compaction step increased the specimen height by 5 mm until the final height was reached.

For the experimental group, mechanical vibration was introduced intermittently during the compaction process when the specimen height reached 20, 40, 60, 80, 100, and 120 mm (Fig. 2a). During vibration treatment, a commercial off-the-shelf

https://doi.org/10.5194/egusphere-2026-2115
Preprint. Discussion started: 12 May 2026

handheld vibrator was pressed onto the same punch used for compaction, and the vibration was transmitted to the snow specimen through the punch rather than by direct contact between the vibrator and the snow. Each vibration treatment lasted 60 s, and the vibrator operated at 4000 rpm. During this process, the nominal contact stress transmitted through the punch to the snow surface was manually maintained within 38–42 kPa. The specimen height was checked before and after each vibration treatment, and no obvious change was observed, indicating that the overall specimen density remained essentially unchanged during vibration. After each vibration treatment, layered compaction was resumed until the next scheduled vibration stage or until the specimen reached the final height of 120 mm. The control group was prepared using the same layered compaction procedure and target density, but without vibration treatment. Both groups comprised 12 samples, which were subsequently subjected to isothermal sintering at -10°C for 48 h.

The preparation procedure was standardized as much as possible by controlling the snow source, particle size range, layer thickness, target density, vibration timing, vibration duration, and nominal contact stress range. For each group, 12 replicate specimens were prepared, and the reported results were based on the mean values of these specimens to reduce the influence of specimen-to-specimen variability on the group comparison.

The specific density was selected to align with the study's objective: to investigate the strengthening effect of mechanical vibration—as an isolated variable—on the elastic modulus of compacted Antarctic snow, without altering the density. This consideration is vital because lower-density snow tends to undergo densification during the vibration process. Moreover, the selected density of 0.6 g/cm³ falls within the medium-to-high density range relevant to practical engineering applications (Abele, 1990). The determination of vibration parameters was guided by two key factors. Firstly, the applied stress (38–42 kPa) and vibration frequency (4000 rpm) are consistent with ranges established in previous engineering applications. Secondly, these parameters satisfy the experimental constraint of not altering the density of the compacted Antarctic snow. The sintering temperature of -10°C was selected for two primary reasons. On the one hand, it represents a typical summer temperature in the Antarctic coastal regions. On the other hand, its proximity to the melting point accelerates the snow sintering process, thereby reducing the required waiting time and helping to shorten construction periods in practical engineering.

Figure 3 shows the flowchart of the snow sample preparation and μCT scanning of this study. For μCT scanning, the experimental and control specimens were prepared under the same conditions as the P-wave specimens in terms of snow source, particle size range, target density, compaction method, vibration protocol, and sintering condition. However, unlike the P-wave specimens, which had a size of 50 × 50 × 120 mm, the μCT specimens were prepared with a smaller size of 30 × 30 × 80 mm, because μCT analysis required smaller samples and this size facilitated the subsequent impregnation and cutting procedures. After all samples for μCT scanning were prepared, they were also subjected to isothermal sintering at -10°C for 48 hours. To prevent metamorphism and deformation of sintered snow samples during transportation from the isothermal sintering chamber to the μCT laboratory, this study adopted the casting method proposed by Lombardo et al. (2021) using diethyl phthalate (DEP)-enhanced contrast agents. Following the 48-hour sintering, the samples were cast in -4°C environment (Fig. 2 (b)) and subsequently rapidly frozen at -55°C. For the μCT scans, 12 samples were prepared for each group.

https://doi.org/10.5194/egusphere-2026-2115
Preprint. Discussion started: 12 May 2026

3 Experiment

3.1 P-wave Propagation

In this study, measurements of snow's elastic modulus were conducted following the protocol of P-wave propagation experiment proposed by Gerling et al. (2017). Given the snow sample preparation procedure and the subsequent isothermal sintering at -10℃, this study assumed transversely isotropic symmetry in snow samples (Köchle and Schneebeli, 2014; Löwe et al., 2013; Shertzer and Adams, 2011). Accordingly, the effective stiffness tensor C of the compacted snow has five independent components (Mavko et al., 2009) as follows.

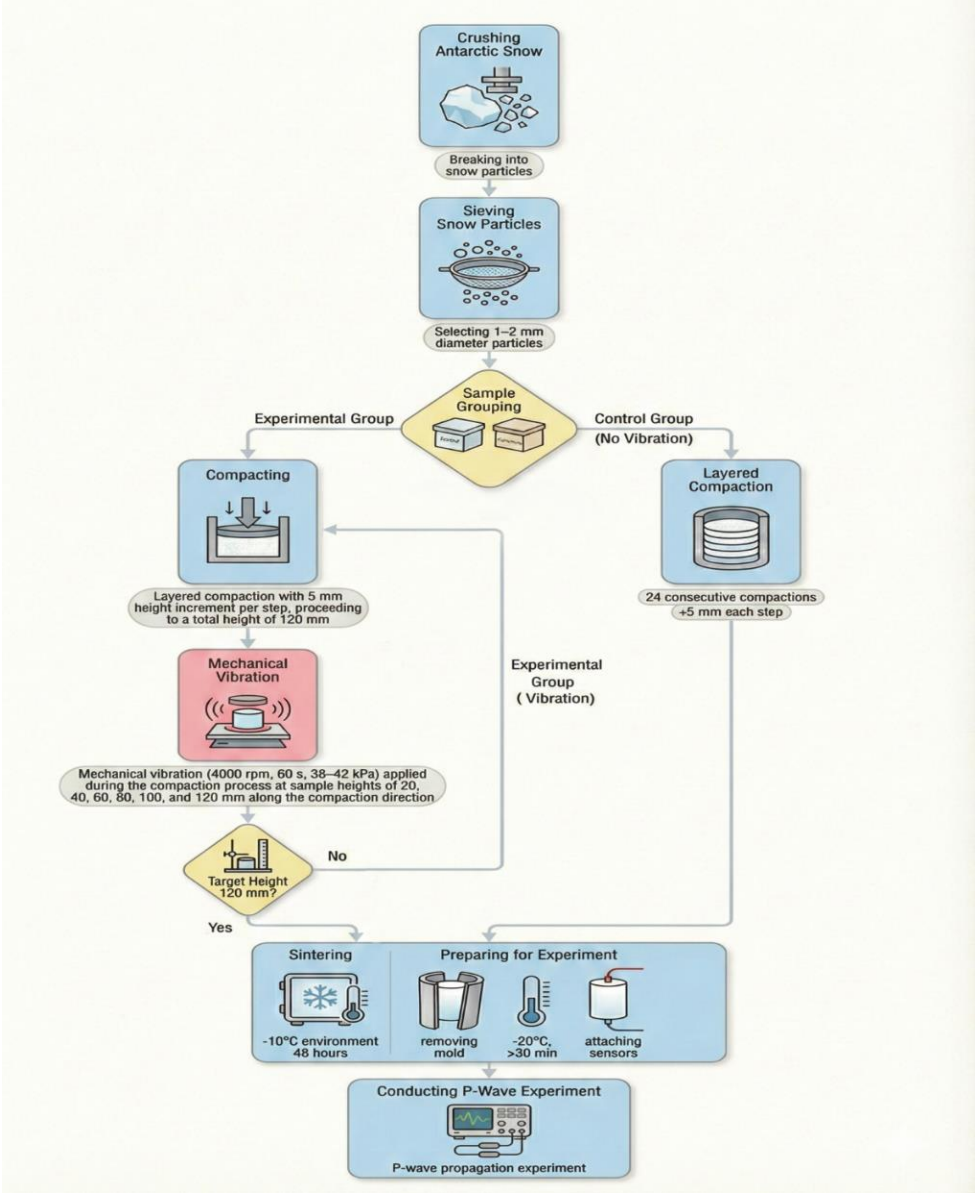

https://doi.org/10.5194/egusphere-2026-2115
Preprint. Discussion started: 12 May 2026

Figure 1: Flowchart of the preparation and P-wave experiment for compacted Antarctic snow.

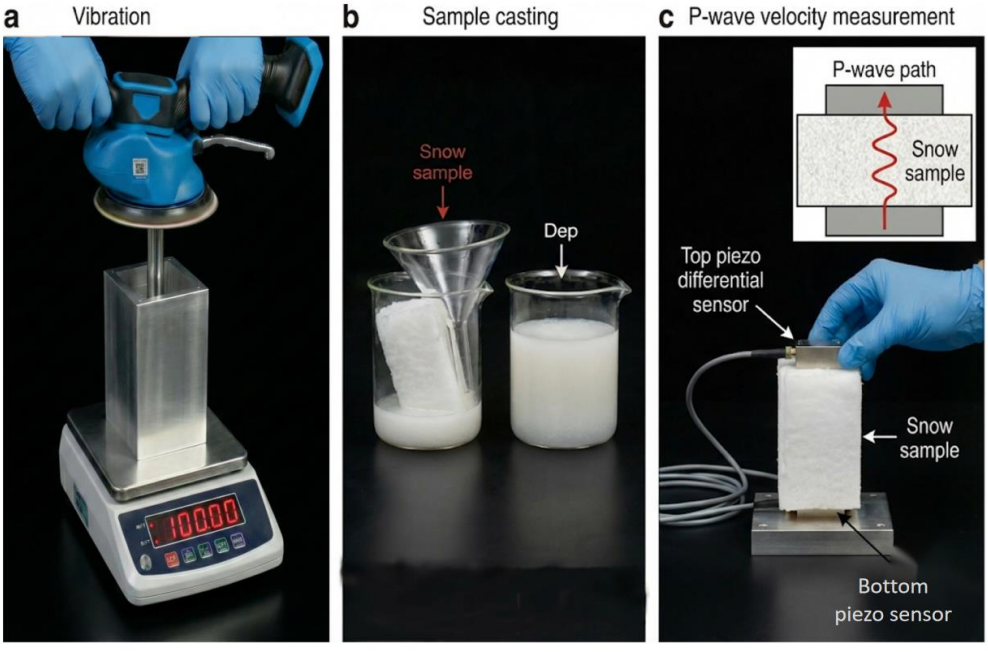

Figure 2: Snow sample preparation and experiment.

$$\boldsymbol{C} = \begin{pmatrix} c_{11} & c_{12} & c_{13} & 0 & 0 & 0 \\ c_{12} & c_{11} & c_{13} & 0 & 0 & 0 \\ c_{13} & c_{13} & c_{33} & 0 & 0 & 0 \\ 0 & 0 & 0 & c_{44} & 0 & 0 \\ 0 & 0 & 0 & 0 & c_{44} & 0 \\ 0 & 0 & 0 & 0 & 0 & c_{66} \end{pmatrix}, c_{66} = \frac{1}{2}(c_{11} - c_{12}) \quad (1)$$

Elastic wave propagation velocity is intrinsically related to wave vector orientation. Following the elastic wave theory for anisotropic media proposed by Tsvankin (1996), the propagation velocity of quasi-longitudinal P-waves can be expressed as a function of the angular deviation θ between the wave vector and symmetry axis

$$v = (c_{11}\sin^2(\theta) + c_{33}\cos^2(\theta) + c_{44} + \sqrt{A})^{\frac{1}{2}}(2\rho)^{-\frac{1}{2}} \quad (2)$$

in terms of

$$A = [(c_{11} - c_{44})\sin^2(\theta) - (c_{33} - c_{44})\cos^2(\theta)]^2 + (c_{13} + c_{44})^2\sin^2(2\theta) \quad (3)$$

where ρ is the snow density. For longitudinal P waves propagating along the axis of symmetry where $\theta = 0$, Equation (2) can be simplified to

https://doi.org/10.5194/egusphere-2026-2115
Preprint. Discussion started: 12 May 2026

$$v = \sqrt{\frac{c_{33}}{\rho}} \tag{4}$$

The elastic modulus c_{33} can be directly determined by measuring the P-wave propagation velocity v along the symmetry axis. Prior to the P-wave propagation experiments, the mold was removed and the samples were placed in a -20°C environment for at least 30 minutes to stabilize the sample temperature. Metal plates were then frozen to the upper and lower surfaces of each sample along the compaction direction. Two broadband differential piezoelectric sensors were mounted on the metal plates. Sensor output signals were amplified by analog preamplifiers and digitized using an 18-bit analog-to-digital converter at a 5 MHz sampling frequency. To ensure optimal contact, silicone grease and spring-loaded pressure were applied to sensor surfaces.

In the experiment, acoustic pulses were generated along the compaction direction by fracturing a pencil lead at the upper metal plate (Fig. 2 (c)). The pulse onset times across channels were autonomously identified using the Akaike Information Criterion (Kurz, 2005), enabling the calculation of wave velocity v along the symmetry axis. The elastic modulus c_{33} was subsequently derived using Eq. (4). For both vibration-treated (experimental group) and non-vibrated (control group) samples, the mean elastic modulus values from 12 parallel samples were adopted as representative values under each experiment condition.

3.2 Microstructure reconstruction via µCT scanning

For µCT scanning, each cast snow sample from the experimental and control groups was further cut into 5×5×5mm cubes and imaged using a SKYSCAN 1272 high-resolution X-ray microtomograph. The scan settings were as follows: source voltage 70 kV, source current 141 µA. To shorten the scan duration and minimize the risk of melting of the snow during scanning, projection images were acquired over a 180° rotation around the vertical axis rather than a full rotation. The reconstructed grayscale images were processed using the modified Feldkamp cone-beam algorithm (Feldkamp et al., 1984) together with a Gaussian filter (support 2). Threshold segmentation was then applied to distinguish the ice matrix from pore voxels at a resolution of 8.56 µm, thereby reconstructing the three-dimensional microstructure of the snow samples.

In the subsequent microstructural analysis, a cubic region was selected from each µCT sample for index calculation, and the selected regions from the experimental and control groups were controlled to have the same density (0.6 g/cm³), thereby excluding density differences as a source of variation in the group comparison. For each microstructural index, values from all analysed samples within the same group were further averaged to obtain representative group-level results, thereby reducing the influence of specimen-to-specimen scatter on the comparison between the two groups.

https://doi.org/10.5194/egusphere-2026-2115
Preprint. Discussion started: 12 May 2026

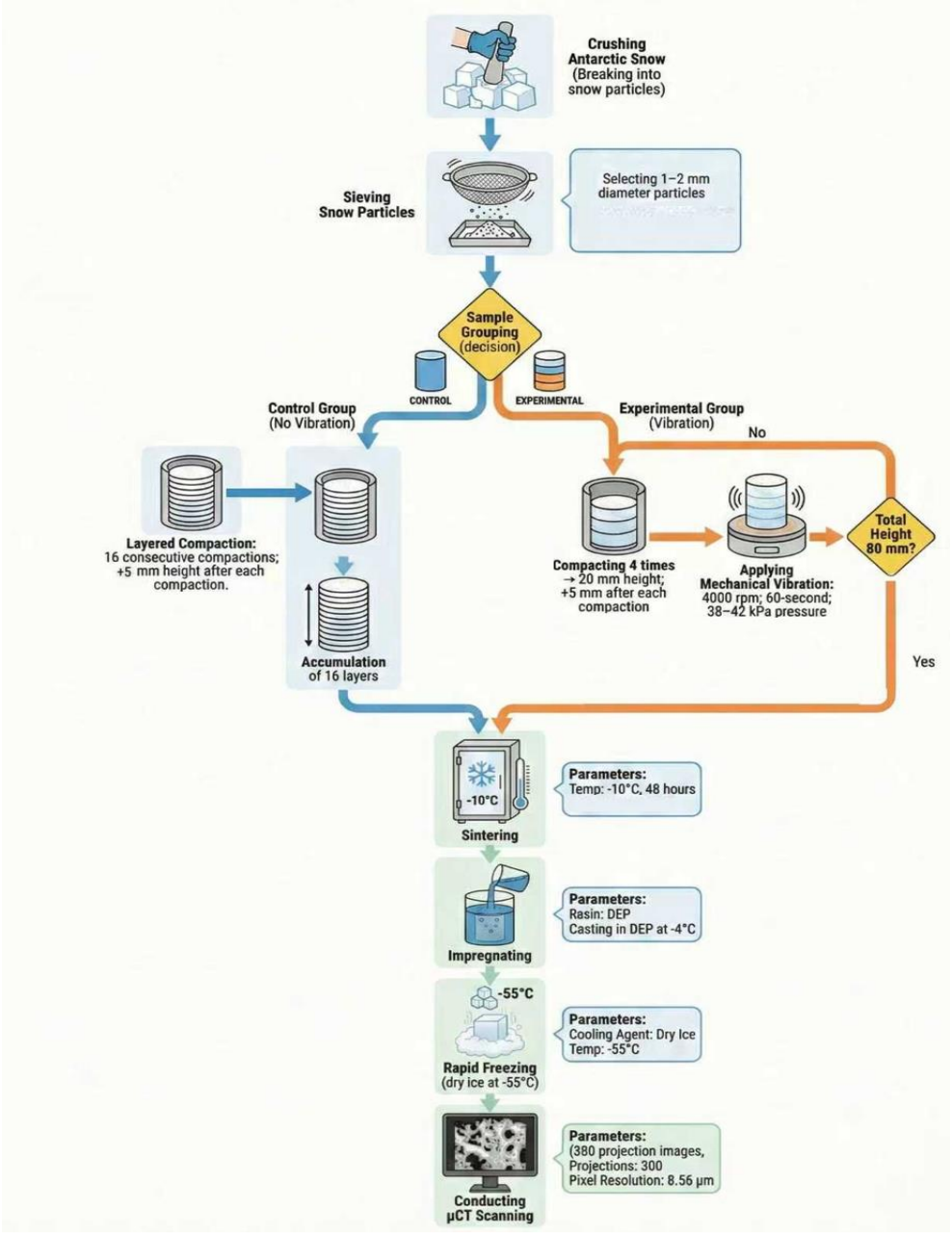

Figure 3: Flowchart of the preparation and µCT scanning for compacted Antarctic snow.

https://doi.org/10.5194/egusphere-2026-2115
Preprint. Discussion started: 12 May 2026

4 Mesoscale index

4.1 Structure and pore thickness

Hildebrand and Rüegsegger (1997) defined local thickness as the diameter of the largest sphere that contains a given point and lies entirely within the phase of interest (Fig. 4). Accordingly, structure thickness is obtained when the phase of interest is the ice matrix, whereas pore thickness is obtained when the phase of interest is the pore space. In snow research, these metrics have been widely used to characterize microstructural evolution during temperature-gradient metamorphism (Schneebeli and Sokratov, 2004; Pinzer, 2009). Compared with grain-based descriptors, structure thickness and pore thickness do not require explicit segmentation of individual grains, and therefore avoid the arbitrariness associated with grain definition in continuous snow microstructures. This advantage is especially important for compacted snow, in which grain boundaries are often difficult to define clearly. Structure thickness characterizes the local geometric size distribution of the ice matrix, whereas pore thickness characterizes the local geometric size distribution of the pore space. Xiao et al. (2026a) further identified structure thickness and directional connectivity as relevant mesoscale indices for parameterizing the elastic modulus of dense snow. Schöttner et al. (2026) also included local thickness among the microstructural descriptors used to interpret the mechanical behavior of weak snow layers. Therefore, structure thickness and pore thickness are adopted in this study to characterize vibration-induced changes in the local geometric distributions of the ice matrix and pore space, respectively, and to help interpret the corresponding variation in elastic modulus.

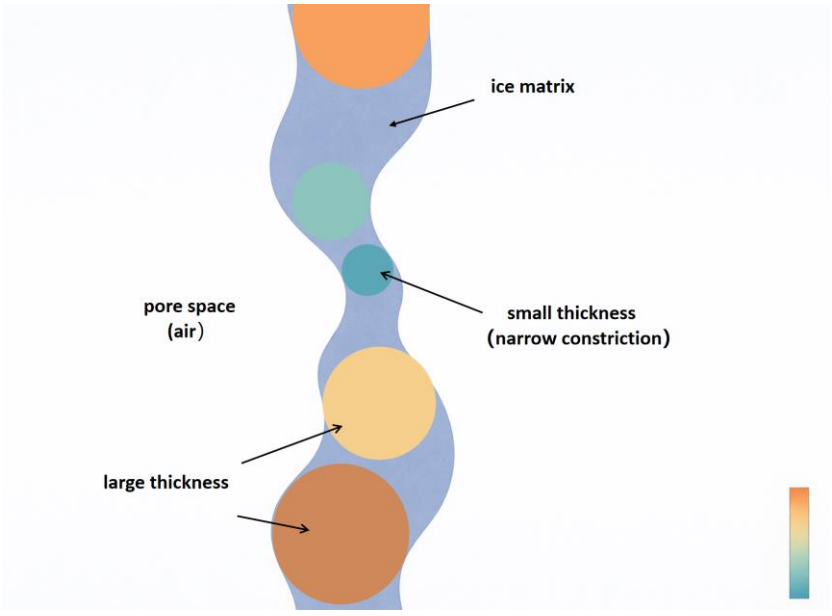

Figure 4: Schematic illustration of local ice-matrix thickness and narrow constrictions in the snow microstructure

https://doi.org/10.5194/egusphere-2026-2115
Preprint. Discussion started: 12 May 2026

4.2 Minimum cut density

Ballard and McGaw (1965) first theoretically introduced the concept of minimum cut density by defining the "effective porosity on failure planes". Ballard and McGaw (1965) and Ballard and Feldt (1965) hypothesized that stress is homogenous and maximal on the minimum cut surface. Hagenmuller et al. (2014) achieved the measurement of this microstructural parameter. They defined the minimum cut surface as the surface with the minimal ice cutting area among all surfaces disconnecting the two opposite faces of the snow sample (Fig. 5), and defined the minimum cut density ρ_{mc} as the ratio of the product of the minimum cut surface area (ice cutting) and ice density to the cross-sectional area perpendicular to the loading direction of the sample, thereby eliminating its volume dependence.

The computation of this mesoscale metric requires no grain definition but retains the concept of bonds as "flow-limiting valves" proposed by Colbeck (1997), while accounting for the anisotropy of ice matrix and the determinant role of narrowed constriction subsets within the ice matrix in governing the macroscopic behaviour of snow samples. Hagenmuller et al. (2014) demonstrated a strong correlation between minimum cut density and elastic modulus, confirming its capability to reveal the influence of microstructural variations on elastic modulus. Schöttner et al. (2026) included minimum cut density in their analysis of the compressive mechanical properties of weak snowpack layers and showed that the minimum cut bond area was among the most informative microstructural descriptors, further supporting the mechanical relevance of critical constrictions within the ice matrix. Thus, it was adopted in this study to analyze the mesoscale mechanism behind vibration-induced effects on snow's elastic modulus.

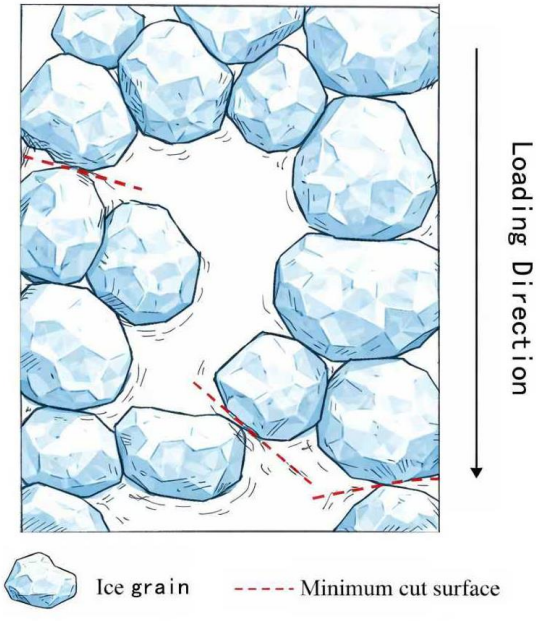

Figure 5: Example of the minimum cut surface.

https://doi.org/10.5194/egusphere-2026-2115
Preprint. Discussion started: 12 May 2026

4.3 Directional connectivity

Xiao et al. (2026a) analyzed the stress distributions within compacted Antarctic snow microstructures and found that load-bearing force chains predominantly concentrate in regions connected to adjacent areas, forming localized yet continuous top-to-bottom force-transmitting channels along the loading direction (Fig. 6). Further examination of parallel and perpendicular cross-sections confirmed that the existence of such connected local force-transmitting channels throughout the microstructure in the loading direction is a necessary condition for the formation of load-bearing force chains. This finding highlights the importance of quantifying the continuity and effectiveness of force transmission along the loading direction. The basis of this type of characterization can be traced to the directional connectivity index proposed by Larsen et al. (2012), which was developed to describe connectivity patterns along a designated direction. However, although this original index effectively captures directional connectivity patterns, later studies showed that it cannot distinguish between mechanically distinct microstructures with similar connectivity configurations. To overcome this limitation, Xiao et al. (2026b) proposed a directional connectivity incorporating the mechanical behavior of load-bearing chains, and adopted this index in the mesoscale analysis of the strengthening effect of mechanical vibration on the uniaxial compressive strength of compacted Antarctic snow. In this index, the voxelized microstructure is represented as a graph, and the contribution of each voxel is evaluated according to its shortest-path distances to the top and bottom boundaries in the loading direction (Fig. 6). In this way, voxels belonging to quasi-linear top-to-bottom force-transmitting paths are assigned greater weights, whereas isolated voxels and mechanically redundant transverse connections contribute little to the final value. Therefore, this directional connectivity index characterizes the continuity and effectiveness of load-bearing paths within the snow microstructure along the loading direction. This interpretation is also consistent with the findings of Schöttner et al. (2026), who showed that snow stiffness is primarily influenced by microstructural features describing the alignment and efficiency of load-bearing paths. Therefore, directional connectivity is adopted in the present study as one of the mesoscale indices to characterize vibration-induced changes in the continuity and effectiveness of force transmission, and to help interpret the corresponding variation in elastic modulus.

https://doi.org/10.5194/egusphere-2026-2115
Preprint. Discussion started: 12 May 2026

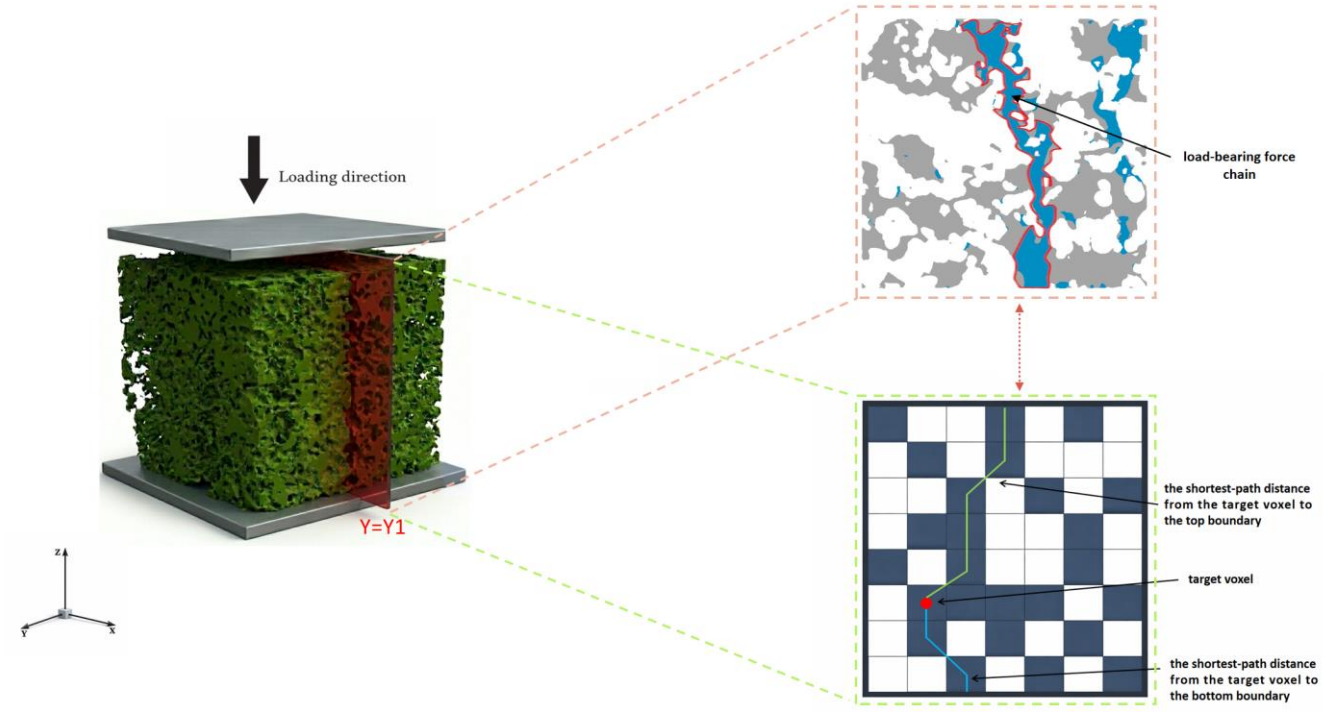

Figure. 6: Schematic illustration of the sectional analysis used to identify load-bearing force chains and calculate directional connectivity (DC). A vertical section at $Y = Y1$ is extracted from the snow microstructure under uniaxial compression along the loading direction. The upper-right panel shows the load-bearing force chain identified on the section, while the lower-right panel illustrates the shortest-path-based calculation of the distance from a target voxel to the top and bottom boundaries for DC evaluation.

5 Results and Analysis

5.1 Macro-scale Elastic Modulus Analysis

The measured elastic modulus for both experimental (12 samples) and control groups (12 samples) are presented in Fig. 7. Experimental group exhibits a mean elastic modulus of 4.201 GPa, compared to 2.294 GPa for control group, i.e., 83.13% enhancement in mean elastic modulus for vibrated samples relative to non-vibrated counterparts. These quantitative results demonstrate the significant strengthening effect of vibratory treatment on the elastic modulus of compacted Antarctic snow.

https://doi.org/10.5194/egusphere-2026-2115
Preprint. Discussion started: 12 May 2026

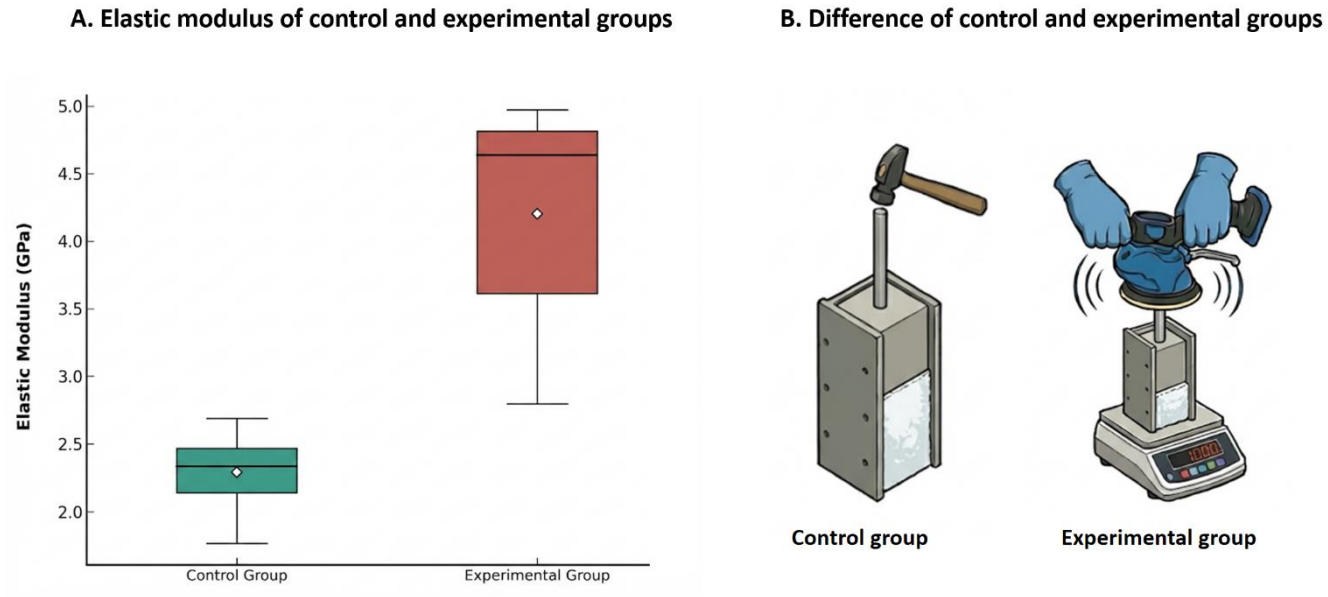

Figure 7: The result of elastic modulus measured by P-wave propagation experiment.

5.2 Mesoscale mechanism analysis

Figure 8 reveals that control group samples contain fewer, larger, and unevenly distributed pores, whereas vibrated samples show smaller pores with uniform spatial distribution.

https://doi.org/10.5194/egusphere-2026-2115
Preprint. Discussion started: 12 May 2026

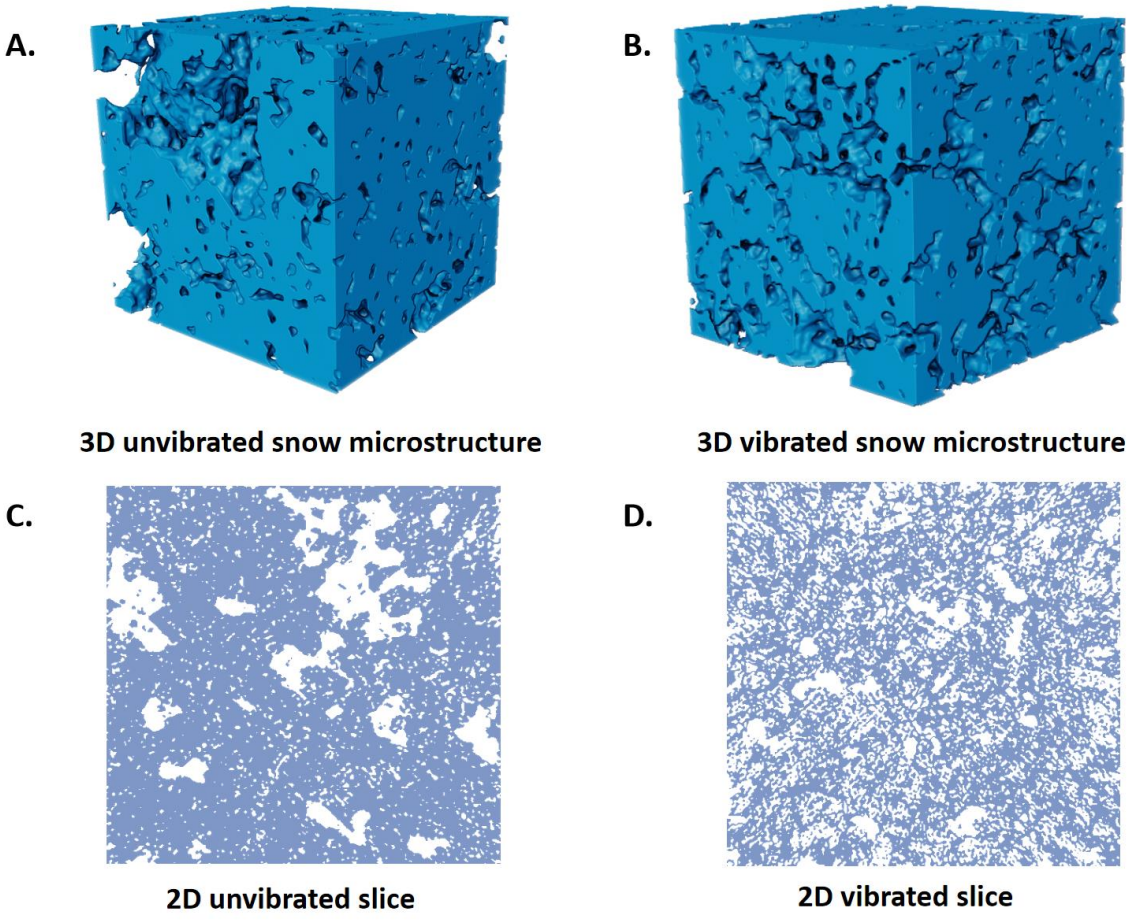

Figure 8: Reconstructed 3D microstructures and 2D slices of snow.

The mean values and standard deviations of structure thickness and pore thickness for both the experimental group and the control group are presented in Fig. 9. The experimental group shows 7.14% lower mean structure thickness (independent samples t-test: p=0.003) and 12.41% lower standard deviation of structure thickness (independent samples t-test: p=0.003) compared to the control group, indicating that the snow samples in the control group displayed greater heterogeneity in ice matrix, with localized regions of larger structure thickness. Similarly, the experimental group shows 13.68% lower mean pore thickness (independent samples t-test: p=0.014) and 30.43% lower standard deviation of pore thickness (independent samples t-test: p=0.015), which indicates that after vibratory treatment, the snow samples in the experimental group exhibit reduced pore sizes and more homogeneous pore distribution. These results are in line with the microstructural homogenization shown in Fig. 8 induced by vibratory treatments. While the large fluctuation in thickness values in the control group aligns with the significant and inevitable heterogeneity in pore distribution resulting from compaction, mechanical vibration serves to mitigate

https://doi.org/10.5194/egusphere-2026-2115
Preprint. Discussion started: 12 May 2026

this variability. By inducing internal particle rearrangement, vibration effectively reduces the extreme fluctuations, leading to a more consistent range of values.

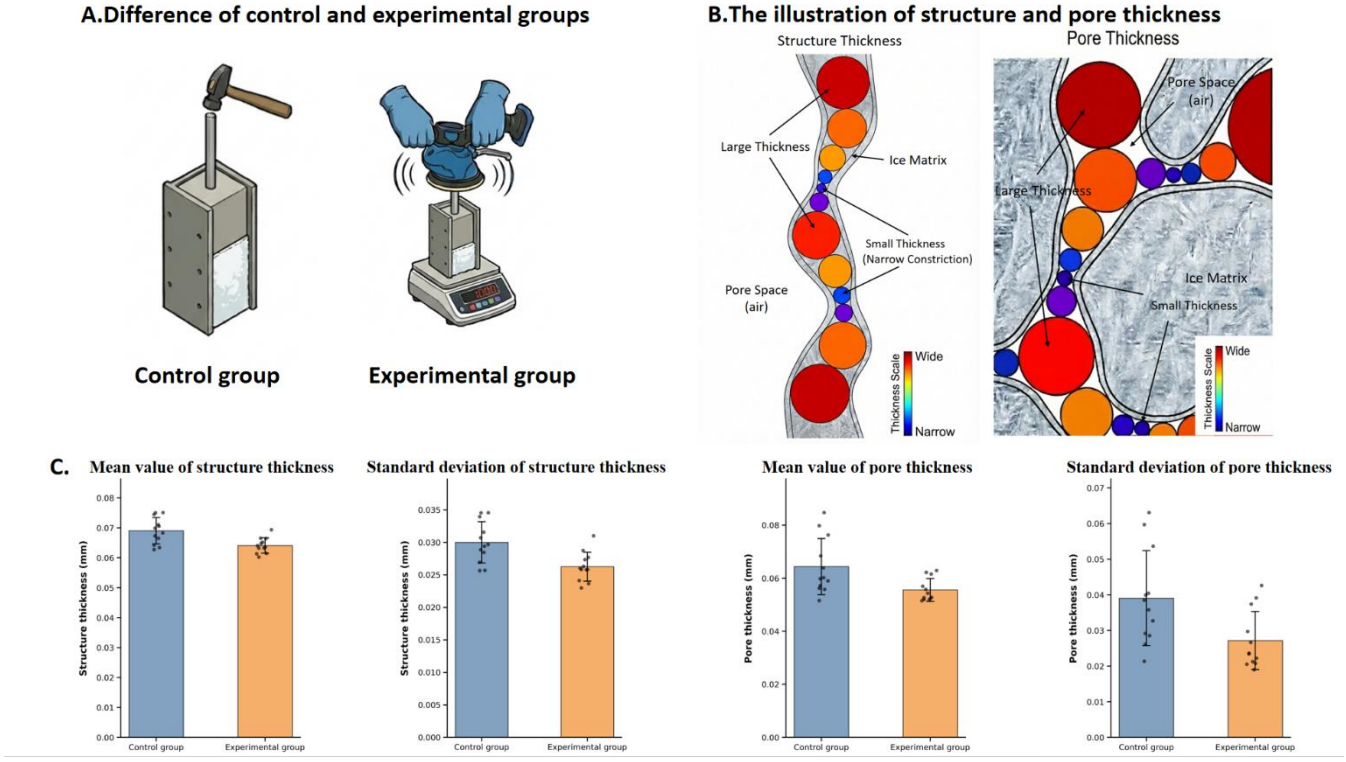

Figure 9: Mean value and Standard deviation of structure and pore thickness.

As shown in Fig. 10, the vibration-treated samples exhibit a mean minimum cut density of 0.505 g/cm^3, while the mean value of non-vibrated control group is 0.425 g/cm^3. The vibration-treated snow samples exhibit an 18.82% higher mean value of minimum cut density compared to untreated snow samples (independent samples t-test: p=0.043). According to Hagenmuller et al. (2014), minimum cut density is defined as an extremal variable designed to identify the weakest cross-section within a structure. In contrast to the spatially averaged bulk density, this indicator—based on the 'weakest link' principle—is highly sensitive to local random defects in the microstructure. Consequently, the results for minimum cut density exhibit significant variability. This indicates that the vibratory treatment enhances the ice cutting area of the minimum cut surface in snow samples by homogenizing the pore distribution.

As shown in Fig. 11, the experimental group exhibits a mean directional connectivity of 0.587, while the mean value of the control group is 0.575. Snow samples subjected to vibratory treatments demonstrate 2.09% higher directional connectivity compared to untreated snow samples (independent samples t-test: p=0.007). Since the density of the microstructures used for calculation in both the experimental and control groups was controlled at 0.6g/cm3, this 2.09% difference can be attributed to the effects of mechanical vibration.

These results confirm that vibratory treatment enhances the load-bearing connectivity of snow samples.

https://doi.org/10.5194/egusphere-2026-2115
Preprint. Discussion started: 12 May 2026

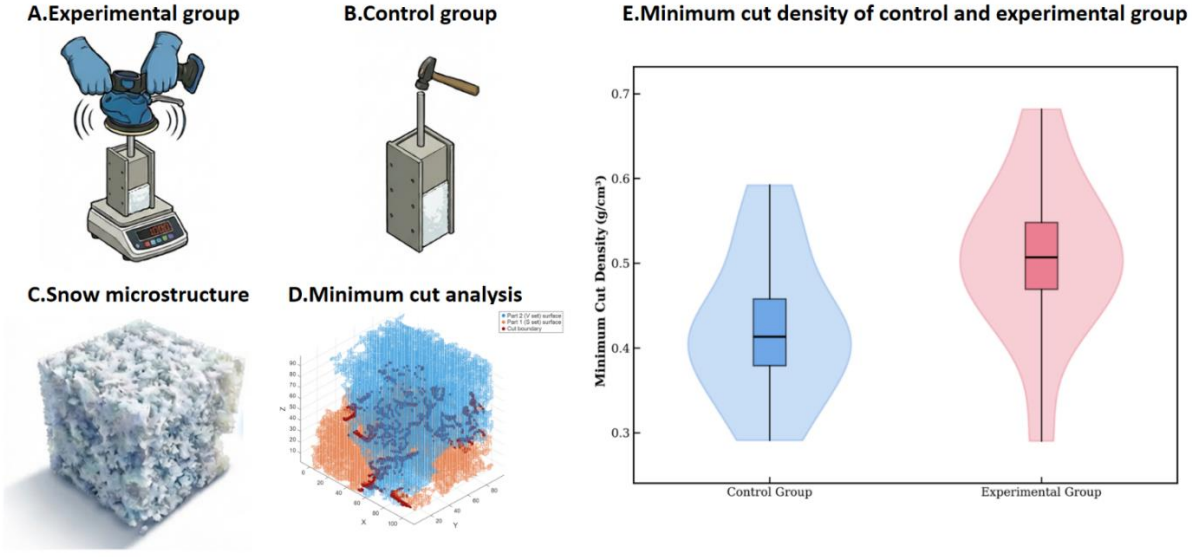

Figure 10: Violin plot of minimum cut density for control and experimental group.

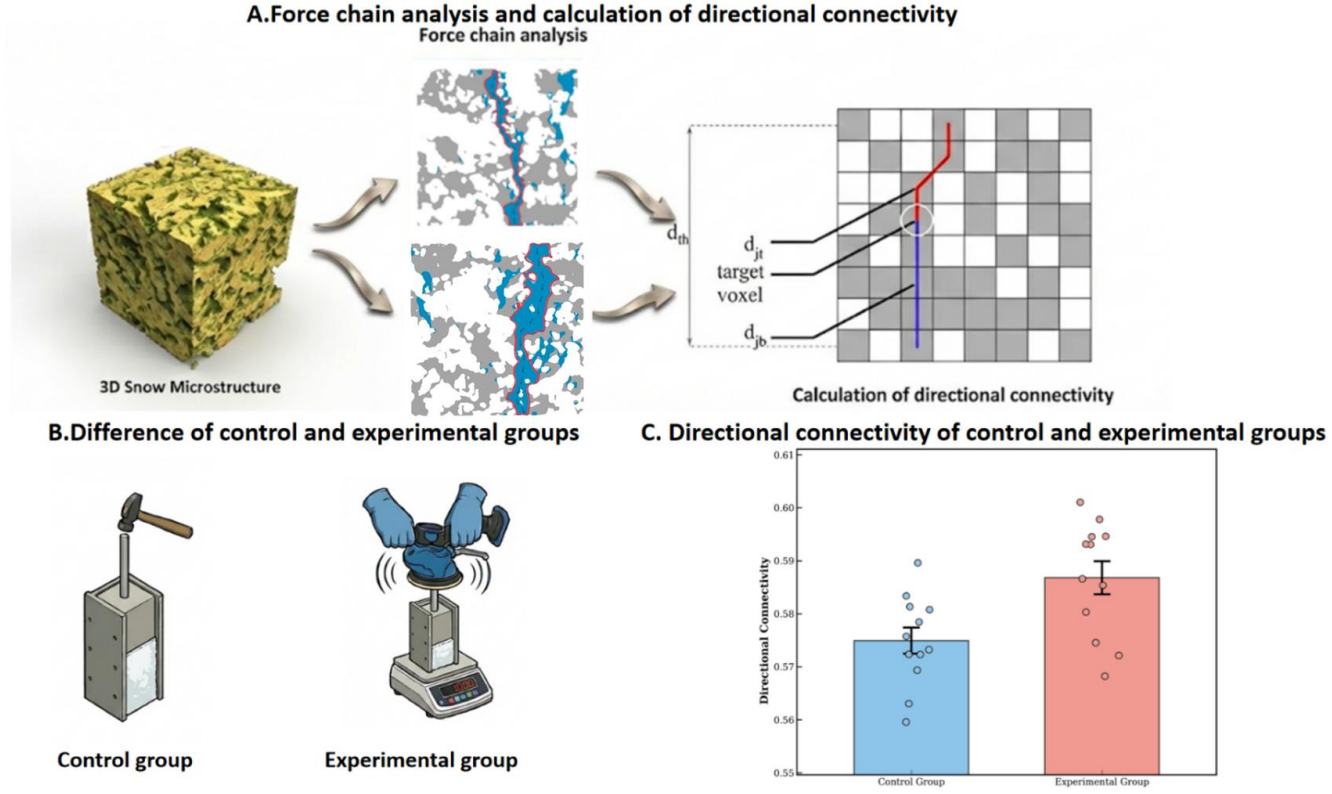

285

https://doi.org/10.5194/egusphere-2026-2115
Preprint. Discussion started: 12 May 2026

Figure 11: Directional connectivity for control and experimental group.

6 Discussion

The increase in elastic modulus observed after mechanical vibration cannot be attributed to density, because the densities of the control and experimental groups were kept identical. The difference therefore indicates that vibration mainly modifies the mesoscale microstructural features governing force transmission. In this study, the four mesoscale indices provide complementary evidence for such a change. Structure thickness and pore thickness describe the geometric distributions of the ice matrix and pore space, whereas minimum cut density and directional connectivity characterize the critical constrictions and the continuity of force-transmitting paths in the loading direction, respectively. Considered together, these descriptors indicate that vibration does not densify the compacted snow, but reorganizes its internal structure in a way that is more favorable for elastic load transfer.

The reductions in the mean values and standard deviations of structure thickness and pore thickness suggest that vibration decreases the heterogeneity of both the solid and pore phases. In the control group, compaction alone leaves relatively large pores and greater local variation in the surrounding ice structure. After vibration, these geometric fluctuations become smaller, indicating a more uniform spatial distribution of the pore space and a more even arrangement of the ice matrix. This interpretation is consistent with the reconstructed microstructures, in which the vibrated samples exhibit smaller and more evenly distributed pores than the non-vibrated samples. Such a reduction in mesoscale heterogeneity is expected to decrease local contrasts in deformation under loading, thereby contributing to a higher effective elastic modulus.

Minimum cut density and directional connectivity further indicate that vibration improves the efficiency of load transfer through the snow microstructure. The increase in minimum cut density suggests that the narrowest effective cross-sections in the loading direction become less restrictive after vibration, while the increase in directional connectivity indicates a more continuous arrangement of force-transmitting paths. These two changes are mechanically consistent with each other: the former reflects the improvement of critical bottlenecks, whereas the latter reflects the continuity of the broader load-bearing network. Their simultaneous increase supports the interpretation that vibration enhances elastic stiffness not by changing bulk density, but by improving the mesoscale architecture through which stresses are transmitted.

On this basis, Fig. 12 is used to schematically illustrate a possible microstructural process induced by vibration in compacted snow. Because layered compaction cannot generate a perfectly uniform structure, the compacted snow initially contains irregularly distributed large pores and locally weak regions, especially around pore edges. Under vibration, the resulting stress oscillations may promote the propagation of microcracks in these weak regions and cause local breakage or detachment of ice particles near pore boundaries. Some of the resulting fragments may then move into adjacent pore space and partially fill the larger voids. As a consequence, the pore structure becomes more uniform and the surrounding ice matrix becomes more favourable for force transmission, while the overall density remains unchanged. This interpretation is consistent with the

https://doi.org/10.5194/egusphere-2026-2115
Preprint. Discussion started: 12 May 2026

observed reductions in the mean values and standard deviations of structure thickness and pore thickness, as well as the increases in minimum cut density and directional connectivity.

The proposed interpretation also helps explain why the timing of vibration is important in practice. If vibration is applied after substantial sintering has already occurred, the existing intergranular bonds may restrict subsequent structural rearrangement. In contrast, applying vibration shortly after compaction is more likely to influence the evolving microstructure. This is qualitatively consistent with the observation of Wuori (1965) that shorter intervals between compaction and vibration lead to greater improvements in snow hardness.

In addition to the microstructural descriptors used in this study, namely structure thickness, pore thickness, minimum cut density, and directional connectivity, the microstructural metric of specific surface area (SSA) was also calculated to further evaluate the effect of vibration on snow microstructure from a geometrical perspective. The results show that the SSA of the experimental group (0.0249 μm^{-1}) was higher than that of the control group (0.0225 μm^{-1}). Since the analysed regions in the experimental and control groups were selected to have the same density, their analysed volume was identical. Therefore, the higher SSA in the experimental group indicates a larger total surface area within the same volume, suggesting that the pore structure in the experimental group became finer and more subdivided, with more small-scale interfaces generated. This result is consistent with the μCT observations in Fig. 8 and also supports the hypothesis proposed in Fig. 12.

It is worth noting that the experimental group exhibited greater scatter in elastic modulus than the control group, whereas the scatter of the thickness-related indices was lower than that of the control group; by contrast, minimum cut density showed greater scatter, and directional connectivity remained at a comparable level in the two groups. One possible reason for this discrepancy is that the macroscopic elastic modulus and the microstructural indices were obtained from two separate sets of specimens. Although the specimen preparation conditions, target density, and sintering time were controlled to be as consistent as possible, some unavoidable variability may still have been introduced between the two sets of samples. However, this variability does not affect the main conclusion of this study, because the comparison between the experimental and control groups was based on the mean values of all samples in each group, thereby accounting for specimen-to-specimen scatter at the group level. On this basis, the combined macroscopic and μCT results still support the conclusion that vibration promotes the fragmentation and rearrangement of snow particles around pores, leading to a more uniform pore size and distribution. The possible origin of the different scatter levels observed between the macroscopic and microstructural indices remains a hypothesis at present and deserves further investigation in future work.

This study examined only one combination of density, sintering time, sintering temperature, and vibration parameters. The present results therefore should be understood as a mesoscale interpretation of vibration-induced stiffening under the specific conditions tested here. Future work is needed to determine how the observed relationships vary with density level, vibration intensity, and sintering conditions.

https://doi.org/10.5194/egusphere-2026-2115
Preprint. Discussion started: 12 May 2026

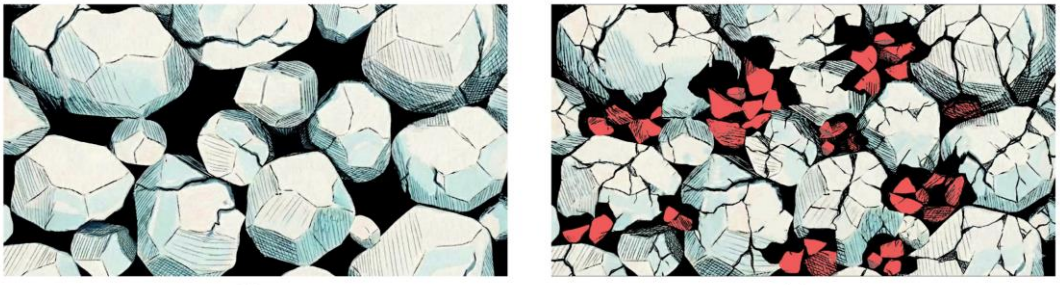

Figure 12: Schematic diagram illustrating the hypothesized mechanism of mechanical vibration.

7 Conclusion

This study investigated the vibration effects on the macroscopic elastic modulus of compacted Antarctic snow and the underlying mesoscale mechanism. The influence of vibratory treatment on the elastic modulus was quantified through P-wave propagation experiments. Microstructural characteristics of the compacted Antarctic snow were obtained from X-ray tomography images.

The results show that:

- At the macroscopic level, under the condition of maintaining a consistent sample density of 0.6 g/cm³, the experimental group exhibits an 83.13% higher average elastic modulus compared to the control group.
- At the mesoscale level, microstructure observations show that vibratory treatment homogenizes the pore distribution within the snow samples. Quantitative analysis demonstrates the following changes in mesoscale indices: For snow samples with identical density (0.6 g/cm³), after vibratory treatment, the mean value of structure thickness decreases by 7.14% (with a standard deviation reduction of 12.41%), the mean value of pore thickness decreases by 13.68% (with a standard deviation reduction of 30.43%), while the minimum cut density increases by 18.82% and directional connectivity improves by 2.09%.

The findings elucidate the mesoscale mechanism underlying vibration-induced improvement in snow's elastic modulus, providing theoretical support for rapid construction techniques of Antarctic snow runways and roads.

Data availability

The data used to generate the figures in this study are available on Zenodo: https://doi.org/10.5281/zenodo.18639193.

Author contribution

https://doi.org/10.5194/egusphere-2026-2115
Preprint. Discussion started: 12 May 2026

FZ and TH completed the experimental setup, produced the figures, and wrote the initial manuscript with input from all co-authors. YW and EX designed the experimental setup.

Competing interests

The authors declare that they have no known competing financial interests or personal relationships that could have appeared to influence the work reported in this paper.

Acknowledgements

The authors would like to express their gratitude for the financial support provided by the National Key Research and Development Project of China under Grant No. 2022YFC2807101.

References

Abele, G.: Snow Roads and Runways, CRREL TR-90-3, Cold Regions Research and Engineering Laboratory, Hanover, NH, USA, 1990.

Ballard, G. and Feldt, E.: A theoretical consideration of the strength of snow, J. Glaciol., 6, 159–170, 1965.

Ballard, G. and McGaw, R. W.: A theory of snow failure, Technical Report, U.S. Cold Regions Research and Engineering Laboratory, Hanover, NH, USA, 1965.

Calonne, N., Flin, F., Geindreau, C., Lesaffre, B., and Rolland du Roscoat, S.: Study of a temperature gradient metamorphism of snow from 3-D images: time evolution of microstructures, physical properties and their associated anisotropy, Cryosphere Discuss., 8, 1407–1451, 2014.

Capelli, A., Kapil, J. C., Reiweger, I., Or, D., and Schweizer, J.: Speed and attenuation of acoustic waves in snow: Laboratory experiments and modeling with Biot's theory, Cold Reg. Sci. Technol., 125, 1–11, 2016.

Chandel, C., Srivastava, P. K., and Mahajan, P.: Micromechanical analysis of deformation of snow using X-ray tomography, Cold Reg. Sci. Technol., 101, 14–23, 2014.

Colbeck, S.: A review of sintering in seasonal snow, CRREL Report, Cold Regions Research and Engineering Laboratory, Hanover, NH, USA, 1997.

Cowin, C.: The relationship between the elastic tensor and the fabric tensor, Mech. Mater., 4, 137–147, 1985.

Feldkamp, L. A., Davis, L. C., and Kress, J. W.: Practical Cone-Beam Algorithm, J. Opt. Soc. Am. A, 1, 612–619, 1984.

https://doi.org/10.5194/egusphere-2026-2115
Preprint. Discussion started: 12 May 2026

Flin, F., Lesaffre, B., Dufour, A., Gillibert, L., Hasan, A., Rolland du Roscoat, S., Cabanes, S., and Pugliese, P.: On the computations of specific surface area and specific grain contact area from snow 3D images, in: Physics and Chemistry of Ice, 321–328, 2011.

Frolov, A. D. and Fedyukin, I. V.: Elastic properties of snow-ice formation in their whole density range, Ann. Glaciol., 26, 55–58, 1998.

Gerling, B., Löwe, H., and Van Herwijnen, A.: Measuring the elastic modulus of snow, Geophys. Res. Lett., 44, 11088–11096, 2017.

Gubler, H.: Determination of the mean number of bonds per snow grain and of the dependence of tensile strength of snow on stereological parameters, J. Glaciol., 20, 329–341, 1978.

Haehnel, R. B., Blaisdell, G. L., Melendy, T., Shoop, S., and Courville, Z.: A snow runway for supporting wheeled aircraft, ERDC/CRREL TR-19-4, U.S. Army Engineer Research and Development Center, Hanover, NH, USA, 2019.

Hagenmuller, P., Calonne, N., Chambon, G., Flin, F., Geindreau, C., and Naaim, M.: Characterization of the snow microstructural bonding system through the minimum cut density, Cold Reg. Sci. Technol., 108, 72–79, 2014.

Hagenmuller, P., Chambon, G., Flin, F., Morin, S., and Naaim, M.: Snow as a granular material: assessment of a new grain segmentation algorithm, Granul. Matter, 16, 421–432, 2014.

Hagenmuller, P., Chambon, G., Flin, F., Wang, X., Lesaffre, B., and Naaim, M.: Description of the snow microstructure as a 3D assembly of grains, International Snow Science Workshop, Grenoble – Chamonix Mont-Blanc, p. 5, 2013a.

Hagenmuller, P., Chambon, G., Lesaffre, B., Flin, F., and Naaim, M.: Energy-based binary segmentation of snow microtomographic images, J. Glaciol., 59, 859–873, 2013b.

Hildebrand, T. and Ruegsegger, P.: A new method for the model independent assessment of thickness in three dimensional images, J. Microsc., 185, 67–75, 1997.

Johnson, D. B.: Efficient algorithms for shortest paths in sparse networks, J. ACM, 24, 1–13, 1977.

Johnson, J. and Schneebeli, M.: Characterizing the microstructural and micromechanical properties of snow, Cold Reg. Sci. Technol., 30, 91–100, 1999.

Köchle, B. and Schneebeli, M.: Three-dimensional microstructure and numerical calculation of elastic properties of alpine snow with a focus on weak layers, J. Glaciol., 60, 705–713, 2014.

Kry, P.: Quantitative stereological analysis of grain bonds in snow, J. Glaciol., 14, 467–477, 1975a.

Kry, P.: The relationship between the visco-elastic and structural properties of fine-grained snow, J. Glaciol., 14, 479–500, 1975b.

Kurz, J. H., Grosse, C. U., and Reinhardt, H. W.: Strategies for reliable automatic onset time picking of acoustic emissions and of ultrasound signals in concrete, Ultrasonics, 43, 538–546, 2005.

Lang, R. M., Blaisdell, G. L., D'Urso, C., Reinemer, G., and Lesher, M.: Processing snow for high strength roads and runways, Cold Reg. Sci. Technol., 25, 17–31, 1997.

https://doi.org/10.5194/egusphere-2026-2115
Preprint. Discussion started: 12 May 2026

Larsen, L. G., Choi, J., Nungesser, M. K., and Harvey, J. W.: Directional connectivity in hydrology and ecology, Ecol. Appl., 22, 2204–2220, 2012.

Lexartza-Artza, I. and Wainwright, J.: Hydrological connectivity: Linking concepts with practical implications, Catena, 79, 146–152, 2009.

Lombardo, M., Schneebeli, M., and Löwe, H.: A casting method using contrast-enhanced diethylphthalate for micro-computed tomography of snow, J. Glaciol., 67, 847–861, 2021.

Löwe, H., Riche, F., and Schneebeli, M.: A general treatment of snow microstructure exemplified by an improved relation for thermal conductivity, The Cryosphere, 7, 1473–1480, 2013.

Marshall, H. and Johnson, J. B.: Accurate inversion of high-resolution snow penetrometer signals for microstructural and micromechanical properties, J. Geophys. Res., 114, F04016, 2009.

Mavko, G., Mukerji, T., and Dvorkin, J.: The Rock Physics Handbook, Cambridge University Press, Cambridge, UK, 2009.

Mellor, M.: A review of basic snow mechanics, in: Snow Mechanics, Symposium at Grindelwald 1974, IAHS Publication 114, 251–291, Wallingford, UK, 1975.

Miller, G. R., Cable, J. M., McDonald, A. K., Bond, B., Franz, T. E., Wang, L., Gou, S., Tyler, A. P., Zou, C. B., and Scott, R. L.: Understanding ecohydrological connectivity in savannas: a system dynamics modelling approach, Ecohydrology, 5, 200–220, 2012.

Narita, H.: Mechanical behaviour and structure of snow under uniaxial tensile stress, J. Glaciol., 26, 275–282, 1980.

Petrovic, J. J.: Mechanical properties of ice and snow, J. Mater. Sci., 38, 1–6, 2003.

Pinzer, B. R.: Dynamics of temperature gradient snow metamorphism – microstructural evolution and transport processes, Doctoral thesis, ETH Zurich, Zurich, 2009.

Reuter, B., Proksch, M., Löwe, H., van Herwijnen, A., and Schweizer, J.: On how to measure snow mechanical properties relevant to slab avalanche release, International Snow Science Workshop, Grenoble, France, 7–11, 2013.

Scapozza, C.: Entwicklung eines dichte- und temperaturabhängigen Stoffgesetzes zur Beschreibung des visko-elastischen Verhaltens von Schnee, PhD thesis, ETH Zurich, Zurich, 2004.

Schneebeli, M.: Numerical simulation of elastic stress in the microstructure of snow, Ann. Glaciol., 38, 339–342, 2004.

Schneebeli, M. and Sokratov, S. A.: Tomography of temperature gradient metamorphism of snow and associated changes in heat conductivity, Hydrol. Process., 18, 2655–2665, 2004.

Schöttner, J., Zeller-Plumhoff, B., Hagenmuller, P., Weißgraeber, P., Rosendahl, P.L., Löwe, H., Schweizer, J., van Herwijnen, A., 2026. The influence of snow microstructure on the compressive mechanical properties of weak snowpack layers. Acta Materialia 302, 121657.

Schweizer, J.: Laboratory experiments on shear failure of snow, Ann. Glaciol., 26, 97–102, 1998.

Shertzer, R. H. and Adams, E. E.: Anisotropic thermal conductivity model for dry snow, Cold Reg. Sci. Technol., 69, 122–128, 2011.

https://doi.org/10.5194/egusphere-2026-2115
Preprint. Discussion started: 12 May 2026

Sigrist, C.: Measurement of fracture mechanical properties of snow and application to dry snow slab avalanche release, PhD thesis, ETH Zurich, Zurich, 2006.

Smith, J. L.: The elastic constants, strength and density of Greenland snow as determined from measurements of sonic wave velocity, Research Report 167, U.S. Cold Regions Research and Engineering Laboratory, Hanover, NH, USA, 1965.

Srivastava, P. K., Chandel, C., Mahajan, P., and Pankaj, P.: Prediction of anisotropic elastic properties of snow from its microstructure, Cold Reg. Sci. Technol., 125, 85–100, 2016.

Srivastava, P. K., Mahajan, P., Satyawali, P. K., and Kumar, V.: Observation of temperature gradient metamorphism in snow by X-ray computed microtomography: measurement of microstructure parameters and simulation of linear elastic properties, Ann. Glaciol., 50, 73–82, 2010.

Theile, T. and Schneebeli, M.: Algorithm to decompose three-dimensional complex structures at the necks: tested on snow structures, IET Image Process., 5, 132–140, 2011.

Torquato, S.: Effective stiffness tensor of composite media .1. Exact series expansions, J. Mech. Phys. Solids, 45, 1421–1448, 1997.

Tsvankin, I.: P-wave signatures and notation for transversely isotropic media: An overview, Geophysics, 61, 467–483, 1996.

Wainwright, J., Turnbull, L., Ibrahim, T. G., Lexartza-Artza, I., Thornton, S. F., and Brazier, R. E.: Linking environmental regimes, space and time: Interpretations of structural and functional connectivity, Geomorphology, 126, 387–404, 2011.

Wang, L., Zou, C., O'Donnell, F., Good, S., Franz, T., Miller, G. R., Caylor, K. K., Cable, J. M., and Bond, B.: Characterizing ecohydrological and biogeochemical connectivity across multiple scales: a new conceptual framework, Ecohydrology, 5, 221–233, 2012.

Wang, X., Gillibert, L., Flin, F., and Coeurjolly, D.: Curvature-driven volumetric segmentation of binary shapes: an application to snow microstructure analysis, International Conference on Pattern Recognition, IEEE Computer Society, 742–745, 2012.

Wautier, A., Geindreau, C., and Flin, F.: Linking snow microstructure to its macroscopic elastic stiffness tensor: A numerical homogenization method and its application to 3-D images from X-ray tomography, Geophys. Res. Lett., 42, 8031–8041, 2015.

Wuori, A. F.: Testing of a vibratory snow compactor, Special Report 55, U.S. Cold Regions Research and Engineering Laboratory, Hanover, NH, USA, 1965.

Xiao E. Z., Wang H., Ding J. B., Tang X. Y., Sun B., Yin Z. X., Han T., and Wang Y. H.: Mesoscale mechanical responses corresponding to the elastic moduli of compacted Antarctic snow near Zhongshan Station, International Journal of Solids and Structures, 327, 113810, 2026a.

Xiao E. Z., Han T., Zhang Q. M., Yin Z. X., Wang H., Hu B., Tang X. Y., Sun B., Zhang F., Wang Y. H.: Vibration effects on the uniaxial compressive strength of compacted Antarctic snow, Cold Regions Science and Technology, 243, 104779, 2026b.

Yuan, H., Lee, J. H., and Guilkey, J. E.: Stochastic reconstruction of the microstructure of equilibrium form snow and computation of effective elastic properties, J. Glaciol., 56, 405–414, 2010.

https://doi.org/10.5194/egusphere-2026-2115
Preprint. Discussion started: 12 May 2026

Zysset, P. K.: A review of morphology–elasticity relationships in human trabecular bone: theories and experiments, J. Biomech., 36, 1469–1485, 2003.